MOLECULAR AND CELLULAR BIOLOGY, Sept. 1986, p. 3023–3033
0270-7306/86/093023-11$02.00/0

Vol. 6, No. 9

Genomic Hypomethylation and Far-5′ Sequence Alterations Are Associated with Carcinogen-Induced Activation of the Hamster Thymidine Kinase Gene

FREDERIC G. BARR, SRIDHARAN RAJAGOPALAN, CRAIG A. MACARTHUR, AND MICHAEL W. LIEBERMAN*

Department of Pathology, Fox Chase Cancer Center, Philadelphia, Pennsylvania 19111

Received 18 February 1986/Accepted 13 May 1986

We have investigated the mechanism of activation of an inactive but functionally intact hamster thymidine kinase (TK) gene by the chemical carcinogen *N*-methyl-*N*′-nitro-*N*-nitrosoguanidine. Following carcinogen treatment of TK$^-$ RJK92 Chinese hamster cells, aminopterin-resistant (HAT^r) colonies appeared at a frequency 50-fold higher than in untreated controls. More than 80% of these HAT^r variants expressed TK enzymatic activity and were divided into high- and low-activity classes. In all TK$^+$ variants, TK expression was correlated with demethylation in the 5′ region of the *TK* gene and the appearance a 1,400-nucleotide TK mRNA. Using high-performance liquid chromatography to measure the level of genomic methylation, we found that four of five high-activity lines demonstrated extensive genomic hypomethylation (approximately 25% of normal level) that was associated with demethylation of all *TK* gene copies. Restriction endonuclease analysis of 15 low-activity lines revealed four instances of sequence alterations in the far-5′ region of the *TK* gene and one instance of a tandem low-copy amplification. In these lines, the structurally altered gene copy was demethylated. Thus, we propose that a chemical carcinogen can activate *TK* expression by several different mechanisms. Focal demethylation with or without gene rearrangement was associated with low TK activity, whereas demethylation throughout the genome was associated with high TK activity.

Although numerous experimental models have demonstrated the ability of chemicals to initiate carcinogenesis (6), the genotypic changes and alterations in gene expression which constitute the initiated state remain unknown. As one approach to these problems, workers in many laboratories have used cell culture systems to investigate how a chemical carcinogen can alter gene expression. Some investigations focused on the ability of carcinogens to mutate an active gene and thereby inactivate gene expression or modify the gene product (10, 18, 26). Recent evidence, however, has expanded the repertoire of carcinogen-induced alterations to include amplification of active genes (34) and activation of quiescent genes (15, 23, 24).

Our laboratory has been investigating carcinogen-induced activation of quiescent genes. To select model systems in which an inactive gene is functionally intact and potentially expressible, we have focused on the class of inactive genes which can be activated by 5-azacytidine (azaCyd), an agent which alters gene expression by epigenetic perturbations presumably related to inhibition of DNA methylation and not by a mutational mechanism (32). The general significance of this class of inactive genes is demonstrated by the occurrence of azaCyd-activatable genes and developmental programs in a variety of cell types (16, 23). One such set of inactive genes is the metallothionein family in mouse S49 T-lymphoma cells; we have previously reported that chemical carcinogens and UV radiation treatment of these cells will activate one or both metallothionein genes and thereby induce cadmium resistance (23, 24).

To explore the generality and diversity of events associated with carcinogen-activated gene expression, we have examined the effect of carcinogen treatment on the inactive thymidine kinase (TK) gene in RJK92 cells, a Chinese hamster fibroblast line. The RJK92 line was derived by exposing TK$^+$ V79 cells to gradually increasing concentrations of bromodeoxyuridine (4, 13). Following treatment with azaCyd, RJK92 cells revert at a very high frequency to the TK$^+$ phenotype (12), indicating that the *TK* gene in RJK92 cells is inactive but functionally intact and potentially expressible. Preliminary reports have suggested that carcinogen treatment of RJK92 and similar lines can induce aminopterin resistance (HAT^r) and *TK* expression (12, 30). In this paper, we have characterized the changes in *TK* gene expression which follow treatment of RJK92 cells with the alkylating carcinogen *N*-methyl-*N*′-nitro-*N*-nitrosoguanidine (MNNG). Furthermore, we have identified changes in hamster DNA associated with *TK* gene activation.

MATERIALS AND METHODS

Cell culture. RJK92 cells (provided by T. Caskey) and carcinogen-induced variants were grown in complete medium as previously described (12). The medium was supplemented with HAT (100 μM hypoxanthine, 0.4 μM aminopterin [Sigma Chemical Co.], and 16 μM thymidine [dThd]) to select HAT^r cells.

Treatment of cells with MNNG and quantitation of effect. After trypsinization of a confluent culture, 2×10^6 RJK92 cells were plated in 75-cm^2 flasks with complete medium and grown for 2 days. The subconfluent monolayers were rinsed with Earle balanced salt solution (EBSS) (Gibco Laboratories), equilibrated with 50 ml of EBSS at 37°C for 30 min, and then treated for 2 h with MNNG (Sigma) which had been dissolved in 0.5 ml of absolute ethanol and then added to the EBSS. After treatment, cells were rinsed with EBSS and then trypsinized; 300 to 1,000 cells were transferred per plate into complete medium for survival measurements. The remaining cells were split 1:2 into complete medium and incubated for 5 days; fresh medium was added as needed. After the 5-day expression period, 300 to 1,000 cells were

* Corresponding author.

transferred per plate into complete medium for plating efficiency measurements, and 2×10^6 cells were transferred per plate into complete medium with HAT for conversion frequency measurements. All plates were incubated for 10 to 14 days with one change of medium and then stained with Wright-Giemsa stain (American Scientific). Stained foci were counted; all small foci were examined microscopically for the presence of intact cells. Survival, plating efficiency (PE), and conversion frequency were calculated from the following equations: plating efficiency = (unselected foci)/(cells added); survival = (surviving foci)/[(cells added)(PE for untreated cells)]; and conversion frequency = (selected foci)/[(cells added)(PE for treated cells)]. These conditions and calculations eliminate any possible quantitative contribution from the seeding of colony-forming units in liquid medium during the 10- to 14-day incubation period, as demonstrated by the statistically indistinguishable conversion frequencies derived from soft agar versus liquid plating (data not shown). In addition, we have determined that, under our conditions, the high density of dying cells does not affect the number of surviving cells (data not shown).

To isolate and expand a variant colony, the colony was removed from an unstained plate with a sterile swab and transferred to a flask containing complete medium. The HAT^r variants described in this paper originated from one culture of RJK92 cells treated with 5 μM MNNG and another culture treated with 10 μM MNNG.

Cell growth standardization and harvest. To standardize cell growth conditions prior to harvest for enzymatic or mRNA assay, 2.5×10^4 to 5×10^4 cells per cm^2 were plated in complete medium (with HAT for resistant lines) and grown for 48 h. Following trypsinization, 1.2×10^4 to 2.4×10^4 cells per cm^2 were plated, grown for 48 h, and harvested. Because the growth rates of the cell lines were not uniform, the number of cells plated at each passage was adjusted within the stated range so that the lines reached comparable degrees of confluence at harvest. For cell harvest, cells were scraped into 10 ml of 0.9% NaCl, sedimented by centrifugation (200 × *g*, 10 min), suspended in 0.9% NaCl, and resedimented.

Enzymatic assay for TK. Soluble extracts were prepared by lysis of the cell pellet in 0.25 to 1.0 ml of extraction buffer (1% Triton X-100, 10 mM 2-mercaptoethanol, 50 mM KH_2PO_4, pH 7.0), followed by freezing at −70°C, thawing, and centrifugation (15,000 × *g*, 10 min, 4°C) (7). The protein content of the extracts was determined by the Bio-Rad protein assay with gamma globulin as a standard.

TK enzyme activity was determined in a radioisotope-DEAE filter-binding assay (R. G. Fenwick, personal communication). The assay mixture contained 10 μl of assay buffer (250 mM Tris, pH 7.4, 25 mM $MgCl_2$), 10 μl of 25 mM ATP, 5 μl of [^{3}H]dThd (Amersham; 1 mCi/ml, 44 Ci/mmol, or diluted with cold dThd to 0.9 mCi/ml, 6 Ci/mmol), and 5 μl of water. After a 10-min preincubation at 37°C, 20 μl of a cell extract (2 mg of protein per ml) was added; 10-μl portions were withdrawn at 10-min intervals from 0 to 30 min and spotted on DE81 filters (Whatman). After 30 s, each filter was dropped in 95% ethanol and then washed three times in ethanol at the completion of the assay. The filters were then dried and the radioactivity was eluted by incubation in 0.5 M NaCl–1 N HCl for 30 min. Following quantitation by liquid scintillation counting, enzyme activity was calculated from the linear regression of the data points and normalized for the specific activity (moles per counts per minute) of the assay mixture. Under these assay conditions, ATP and [^{3}H]dThd were determined to be in substrate excess, and the activity was linear with respect to time and protein (data not shown).

Plasmids. All plasmids were generously provided by J. Lewis. Plasmids p5.5 and p5.2 contain 3 kilobases (kb) from the 5′ end and 5 kb from the 3′ end, respectively, of the hamster *TK* gene (Fig. 1A). Plasmids p9S and p9B contain the first 350 base pairs (bp) and the remaining 900 bp, respectively, of the hamster *TK* cDNA (Fig. 1B). Fragments were isolated from these plasmids by the glass powder technique (35) and were nick translated as described previously (29).

Northern and Southern blot analyses. Total RNA was isolated from the cell pellet by guanidinium isothiocyanate-CsCl centrifugation (25). RNA samples were denatured with glyoxal and dimethyl sulfoxide, electrophoresed in 1.5% agarose gels in 10 mM NaH_2PO_4, pH 7.0, and blotted to nitrocellulose (25). Genomic DNA was isolated from the cell lines as described previously (3). DNA samples were digested with 2 to 7 U of restriction enzyme per μg of DNA for 6 to 8 h, electrophoresed in 0.5 to 1.5% agarose gels, and blotted to nitrocellulose (25). Northern and Southern blots were baked, prehybridized, hybridized to ^{32}P-labeled, nick-translated probes, washed, and exposed as described previously (29).

Quantitation of genomic methylation by HPLC. Cell lines were labeled during exponential growth with 250 nCi of [6-^{3}H]deoxycytidine (dCyd) (5 to 6 Ci/mmol; Moravek Biochemicals) per ml for 20 h. In TK^+ cell lines, the conversion of labeled dCyd to dThd was reduced by adding 100 μM dThd to the medium 3 h prior to the addition of the [6-^{3}H]dCyd. The radioactivity was chased with unlabeled medium, and the cells were incubated for 24 h. Genomic DNA was isolated and digested to nucleosides with DNase I, snake venom phosphodiesterase, and alkaline phosphatase (3). Nucleosides were fractionated by high-performance liquid chromatography (HPLC) and quantitated by liquid scintillation counting as described previously (17, 20).

RESULTS

Carcinogen induction of HAT^r. We treated subconfluent RJK92 cultures in serum-free EBSS with MNNG, a direct-acting alkylating carcinogen (1). The treated cells were passaged to stimulate replication and then incubated in complete medium for a 5-day expression period. (This period probably allows for fixation of lesions and for changes in gene expression to occur and the associated products to accumulate or diminish.) The cells were then plated in medium containing HAT, and the fraction of HAT^r cells was determined. To correct for differences in survival and for any propensity to seed colony-forming units during the 10- to 14-day incubation period, this fraction was normalized for the plating efficiency of each experimental population. At a dose of 1 μM MNNG (80% survival), there was a greater than 20-fold increase in the frequency of HAT^r variants compared with the spontaneous frequency (approximately 1 HAT^r cell/10^6 RJK92 cells) (Fig. 2). At 5 μM MNNG (20% survival), the increase compared with the spontaneous level was greater than 50-fold.

To determine whether the MNNG-induced increases in the HAT^r frequency represented induction of new HAT^r variants or selection of preexisting variants (23, 24), we treated RJK92 cells and cells from six HAT^r lines with MNNG and compared survival and growth rates. The magnitude of the selective survival and growth advantage of HAT^r cells (up to 1.6-fold after treatment with 5 μM MNNG

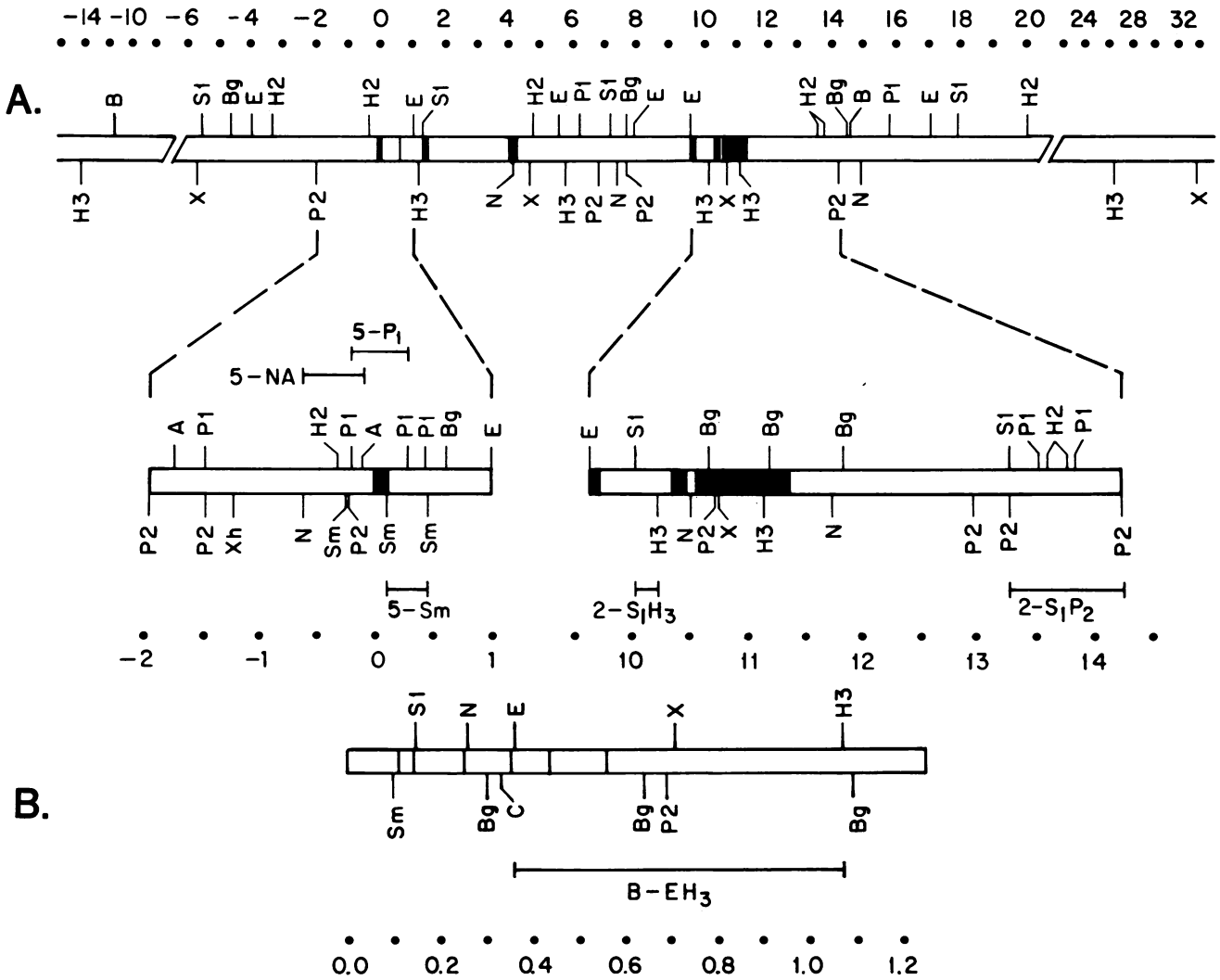

FIG. 1. Structure of the Chinese hamster *TK* gene (A) and *TK* cDNA (B). The two expanded regions correspond to the available cloned sequences (plasmids p5.5 and p5.2); these two regions and the cloned cDNA were mapped by measurement of ethidium bromide-stained bands. Restriction sites for the remainder of the gene were located by Southern blot hybridization analysis. The fragments used as hybridization probes are shown as line segments above and below the cloned regions. The locations of the exons (solid boxes in A and open boxes in B) have been tentatively mapped by comparison of the restriction maps with the cDNA sequence and mapping data of J. Lewis (22; personal communication). Although the approximate location of the second exon is shown, it has not been precisely mapped because of the lack of restriction enzyme sites in this exon. The numerical scale represents distances (in kilobases) from the approximate origin of transcription. Abbreviations: A, *Apa*I; B, *Bam*HI; Bg, *Bgl*I; C, *Cla*I; E, *Eco*RI; H1, *Hha*I; H2, *Hin*cII; H3, *Hin*dIII; M, *Msp*I-*Hpa*II; N, *Nco*I; P1, *Pst*I; P2, *Pvu*II; S1, *Sst*I; S2, *Sst*II; Sm, *Sma*I; X, *Xmn*I; Xh, *Xho*I.

and a 5-day expression period) was insufficient to explain the 20- to 50-fold MNNG-induced increase in HAT^r derivatives of RJK92 (data not shown). We conclude that the increased HAT^r frequency results from induction of new HAT^r variants.

We examined the stability of the MNNG-induced HAT^r phenotype by maintaining five cell lines in HAT-free medium and assaying periodically for HAT^r during a 7-week period (approximately 60 cell generations). For all five lines, the HAT^r phenotype remained quantitatively stable (0.9 to 1.0 HAT^r cells per total cells) during the period examined (data not shown).

Enzymatic analysis of *TK* expression. The relationship of MNNG-induced HAT^r to *TK* expression was determined by enzymatic analysis of cell lines derived from HAT^r colonies induced with 5 or 10 μM MNNG. At an early stage in the growth of these cell lines (10 to 17 days after the colonies were picked), soluble extracts were prepared from subconfluent cultures and assayed for TK enzymatic activity. The background for this assay is 0.0 to 0.4 U (where 1 U = 1 fmol of TMP/min per μg of protein); this background may result from statistical scatter, nonspecific binding of labeled dThd, and low levels of mitochondrial TK (12). More than 80% (22 of 27) of the MNNG-induced HAT^r cell lines (Fig. 3A) and all (3 of 3) the spontaneous HAT^r lines (data not shown) expressed detectable TK activity, which ranged from 2 to 90 U. For comparison, we determined that the TK activity in a wild-type line of V79 Chinese hamster cells was approximately 65 U.

When the initial soluble extracts were prepared for the TK assay (Fig. 3A), the cell lines were relatively young and differed considerably in growth rate and thus in the degree of confluence at harvest. Because *TK* expression varies during the cell cycle and diminishes when cells stop dividing (22),

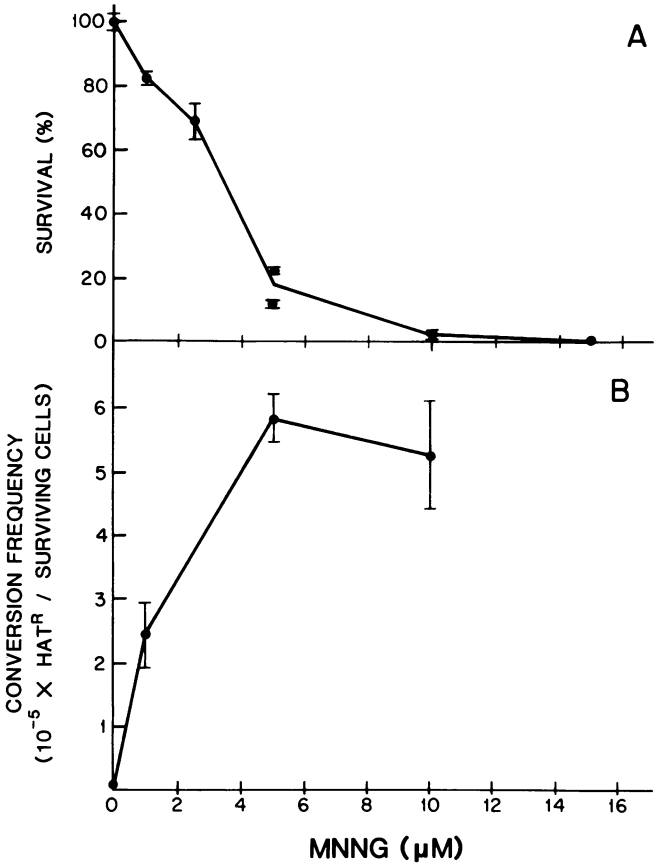

FIG. 2. Dose-response curve for survival (A) and conversion to HAT^r phenotype (B) following treatment of RJK92 cells with MNNG. Each point represents the mean (±SEM) of four or five determinations.

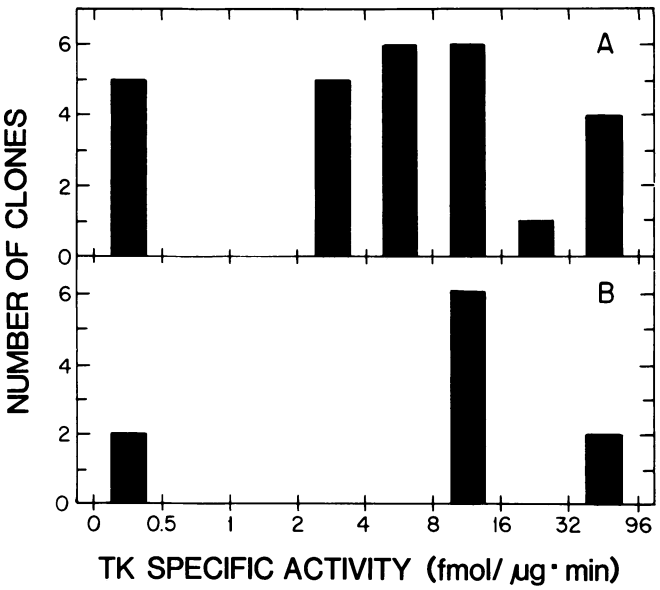

FIG. 3. Specific activity of TK in MNNG-induced HAT^r cell lines derived from RJK92. Shortly after these cell lines were isolated, enzyme activity was assayed in soluble extracts prepared from subconfluent cultures of the HAT^r cell lines (A). Following standardization of the growth and harvest of 10 selected cell lines (two each from the 0 to 0.4 U, 2 to 4 U, 4 to 8 U, 8 to 16 U, and >32 U groups in panel A), new extracts were isolated and the TK activity was assayed again (B).

such differences could lead to artifactual differences in TK specific activity. By standardizing our growth conditions (see Materials and Methods), we detected three discrete classes of TK enzymatic activity. The essential features of this protocol are passage of subconfluent cultures to keep the cultures in continuous division and monitoring of cell number to achieve similar degrees of confluence at harvest. Ten lines (two each from the 0 to 0.4 U, 2 to 4 U, 4 to 8 U, 8 to 16 U, and >32 U activity groups shown in Fig. 3A) were grown according to the standardized protocol and assayed again for TK activity. The activities of lines from the null (0 to 0.4 U) and high (>32 U) groups were comparable to those measured previously (Fig. 3B). However, activities of lines from the middle three groups clustered in the 8 to 16 U range. Thus, HAT^r cell lines can be divided into null (0 to 0.4 U), low (8 to 16 U), and high (>32 U) TK enzymatic activity classes.

Northern blot analysis of RNA. To explore the level of control at which the MNNG-induced activation of *TK* expression occurs, we compared steady-state mRNA levels in RJK92 and HAT^r derivatives by Northern blot analysis. Eleven cell lines (RJK92, two HAT^r TK^- lines, six low-activity TK^+ lines, and two high-activity TK^+ lines) were grown according to the standardized protocol, and total RNA was then isolated from each line. Northern blot analysis of these RNA samples revealed a single band of the size previously reported for hamster TK mRNA (1,400 nucleotides) (22) (Fig. 4). This band was present in all eight TK^+ lines and absent from all three TK^- lines. The correlation of the presence of the 1,400-nucleotide mRNA with the expression of TK enzymatic activity indicates that carcinogen-induced *TK* activation involves changes at the mRNA level.

Methylation analysis of *TK* gene in MNNG-induced TK^+ cell lines. To determine whether alterations in the *TK* gene are

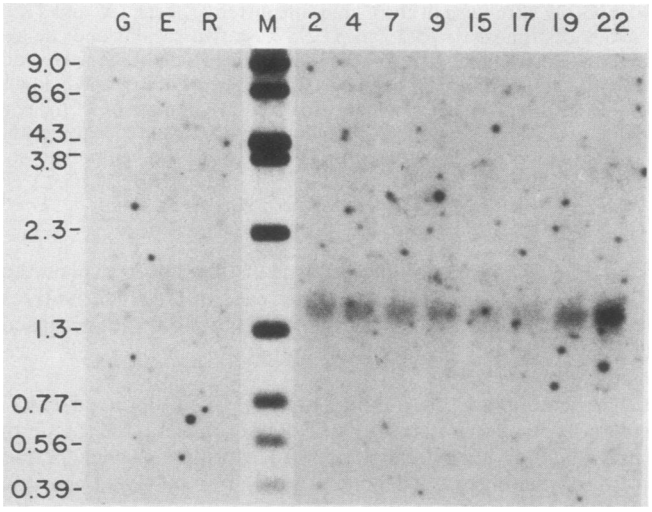

FIG. 4. Northern blot analysis of total RNA isolated from MNNG-induced HAT^r derivatives of RJK92. RNA samples (30 μg) from RJK92 (R), HAT^r TK^- lines E and G, low-activity TK^+ lines 2, 4, 7, 9, 15, and 17, and high-activity TK^+ lines 19 and 22 were denatured, electrophoresed in a 1.5% agarose gel, and blotted. The blot was hybridized to probe B-EH_3 (Fig. 1B). Lane M, Glyoxal (and dimethyl sulfoxide)-denatured end-labeled *Hin*dIII-*Nco*I digest of λ DNA; the sizes (in 10^3 nucleotides) of these fragments are indicated.

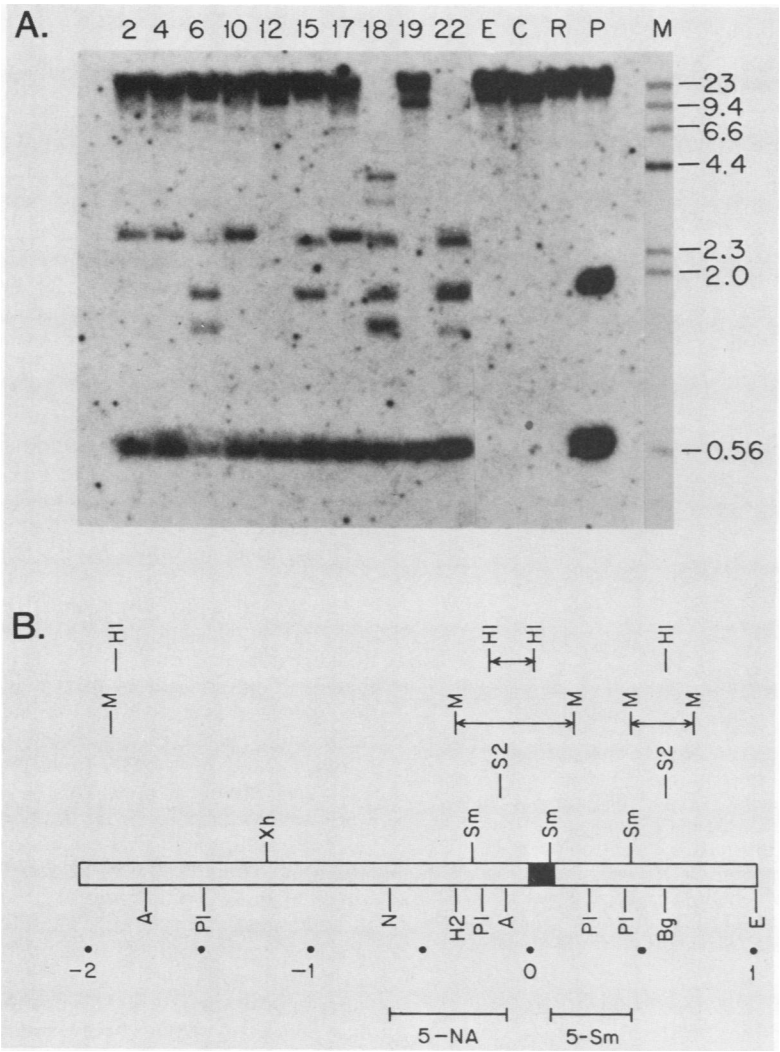

FIG. 5. (A) Methylation analysis of the 5′ *TK* region in MNNG-induced HAT^r derivatives of RJK92. DNA samples (10 μg) from RJK92 (lane R), HAT^r TK$^-$ lines C and E, low-activity TK$^+$ lines 2, 4, 6, 10, 12, 15, and 17, and high-activity TK$^+$ lines 18, 19, and 22 were digested with *Hha*I, electrophoresed in a 1.5% agarose gel, and blotted. This blot was hybridized to probes 5-NA and 5-Sm (B). Lane P, *Hha*I digest of a mixture of plasmid p5.5 (containing the cloned 5′ TK region) and RJK92 DNA. Lane M, End-labeled *Hin*dIII digest of λ DNA. (B) Location of methylation-sensitive restriction enzyme sites in the 5′ region of the hamster *TK* gene. This cloned region was mapped by measurement of ethidium bromide-stained bands. The presence of an arrow between two sites indicates that more sites are present in that region but the resulting fragments were smaller than the limits of resolution of our analysis (<200 bp). The first exon is shown as a solid box, and hybridization probes 5-NA and 5-Sm are shown as line segments below the map. The numerical scale represents distances (in kilobases) from the approximate origin of transcription. Restriction enzyme abbreviations are given in the legend to Fig. 1.

associated with activation, we investigated the methylation status of the 5′ end of the *TK* gene in the MNNG-induced TK$^+$ variants. First, we mapped the sites of five methylation-sensitive restriction enzymes (*Hpa*II, *Hha*I, *Sst*II, *Sma*I, and *Xho*I) in the cloned sequence from the 5′ end of the *TK* gene (Fig. 5B). Because the spacing between *Hha*I sites resulted in two readily detectable fragments, we digested DNA from RJK92, seven low-activity and three high-activity TK$^+$ lines, and two HAT^r TK$^-$ lines with *Hha*I and hybridized the Southern blot with probes 5-NA and 5-Sm (Fig. 5A and B). For an unmethylated control, we used *Hha*I to digest a mixture of the cloned 5′ *TK* sequence (plasmid p5.5) and RJK92 DNA; hybridization with the two probes revealed the fully unmethylated 0.6- and 1.7-kb bands (Fig. 5A, lane P). RJK92 (lane R) and the TK$^-$ cell lines (lanes E and C) showed no demethylation of *Hha*I sites in the 5′ region, whereas all 10 TK$^+$ cell lines demonstrated demethylation (Fig. 5A). We found a similar correlation between demethylation of *Hpa*II sites in the 5′ region and *TK* expression (data not shown). In the *Hha*I blot (Fig. 5A), the 0.6-kb *Hha*I fragment appeared in all TK$^+$ lines, while the 1.7-kb fragment appeared in only a subset of the TK$^+$ lines. These data indicate that the *Hha*I site at position +0.6 and some or all of the *Hha*I sites around position −0.1 were demethylated in all of the TK$^+$ variants (Fig. 5B). In contrast, the *Hha*I site at −1.9 was demethylated in only some of the TK$^+$ lines.

The finding of 1.4- and 2.6-kb demethylated *Hha*I fragments (Fig. 5A) clarified the methylation status of the 5′ *TK* region. The 1.4-kb band was generated by methylation of the *Hha*I site at +0.6 and demethylation at an unmapped downstream site (Fig. 5B). Similarly, the 2.6-kb band could be explained by methylation at the *Hha*I site at +0.6 or −1.9 and demethylation at an unmapped downstream or upstream

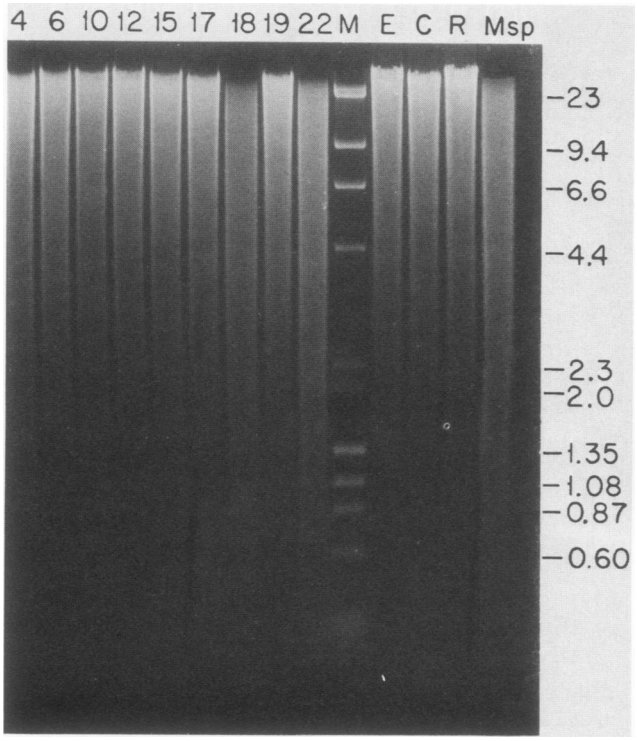

FIG. 6. Methylation analysis of *Hpa*II sites throughout the genome of RJK92 and MNNG-induced HAT^r variants. DNA samples (10 μg) from RJK92 (lane R), HAT^r TK$^-$ lines C and E, low-activity TK$^+$ lines 4, 6, 10, 12, 15, and 17, and high-activity lines 18, 19, and 22 were digested with *Hpa*II and electrophoresed in a 1% agarose gel. Following electrophoresis, the gel was stained with ethidium bromide. Lane Msp contains an *Msp*I digest of RJK92 DNA. Lane M contains a mixture of an *Hin*dIII digest of λ DNA and an *Hae*III digest of φX174 DNA. Sizes are shown in kilobases.

site, respectively. Alternatively, the 2.6-kb fragment could result from methylation of the *Hha*I sites around position −0.1 and demethylation of the sites at +0.6 and −1.9. Therefore, within a given cell line, there is heterogeneity in the methylation status of certain sites in the 5′ region. Such heterogeneity may arise from remethylation of previously demethylated sites during expansion of the TK$^+$ cell lines. Furthermore, these data suggest that only a subset of demethylated sites or a variably demethylated domain may be needed for *TK* expression (28).

In all the low-activity TK$^+$ lines, 5′ demethylation was associated with only a subset of the *TK* gene copies. Following digestion of DNA from seven low-activity lines with *Hha*I, a high-molecular-weight band (about 23 kb) was present in addition to the lower-molecular-weight demethylated bands (Fig. 5A). This high-molecular-weight band corresponded to the highly methylated, presumably inactive copies of the *TK* gene, while the lower-molecular-weight bands originated from the demethylated, presumably active copies. Similar results were also obtained with *Hpa*II digestion (data not shown).

In contrast to the situation in the low-activity TK$^+$ cell lines, no hybridizing band was evident in the high-molecular-weight region (about 23 kb) when DNA from high-activity lines 18 and 22 was digested with *Hha*I (Fig. 5A) or *Hpa*II (data not shown). We conclude that the 5′ region of all copies of the *TK* gene was demethylated in these two high-activity variants. Furthermore, using probes 2-S_1H_3 and 2-S_1P_2 (Fig. 1A), we determined that *Hpa*II sites in the 3′ region of all copies of the *TK* gene were also demethylated in lines 18 and 22 (data not shown).

Analysis of genomic methylation in MNNG-induced TK$^+$ cell lines. To determine whether this demethylation of *Hpa*II and *Hha*I sites was unique to the *TK* gene in the high-activity TK$^+$ lines, we examined the ethidium bromide-stained agarose gel fractionation of the *Hpa*II and *Hha*I digests. The ethidium bromide-stained smears of *Hpa*II fragments from high-activity lines 18 and 22 demonstrated a significant shift towards the lower-molecular-weight region in comparison to the smears from the low-activity TK$^+$ lines and high-activity lines 19 (Fig. 6). In fact, the distribution of *Hpa*II fragments from lines 18 and 22 closely resembled the distribution of fragments from an *Msp*I digest of RJK92 DNA (Fig. 6, lane Msp). These findings suggest that there is extensive demethylation of *Hpa*II sites throughout the genome of lines 18 and 22. Genomewide demethylation of *Hha*I sites was also observed in these two high-activity lines (data not shown). In addition, two previously unexamined high-activity TK$^+$ lines (lines 20 and 21) were digested with *Hpa*II and also demonstrated genomic *Hpa*II hypomethylation (data not shown).

The presence of genomewide demethylation of both *Hpa*II and *Hha*I sites suggested the possibility of demethylation of dCyd residues throughout the genome. We quantitated the methyl-dCyd content of total cellular DNA by radioactive labeling of dCyd residues, digestion of cellular DNA to nucleosides, and HPLC fractionation of the nucleosides (see Materials and Methods). In RJK92 and three low-activity TK$^+$ derivatives, approximately 1.8% of the dCyd residues were methylated (Table 1). In contrast, the fraction of dCyd residues methylated in the high-activity lines 18, 21, and 22 was approximately 0.5%; in these high-activity TK$^+$ derivatives of RJK92, there was a three- to fourfold reduction in the extent of methylation. Therefore, carcinogen treatment of RJK92 cells can lead to extensive demethylation of dCyd residues throughout the genome.

Structural analysis of *TK* gene in MNNG-induced TK$^+$ cell lines. We investigated the possibility of structural alterations such as gene amplification, insertions and deletions, and translocations associated with the *TK* gene in the MNNG-activated TK$^+$ derivatives of RJK92. The transcribed and nearby flanking regions of the *TK* gene were cut into four fragments (from 5′ to 3′: 3.0, 5.0, 5.9, and 2.8 kb) by digesting with *Hin*cII and *Xmn*I and then were identified by probing with 5-NA (Fig. 1A and 7B) and B-EH_3 (Fig. 1B and 7C). The far-5′ and 3′ flanking regions were each examined by digesting with *Hin*dIII (to yield 15.5-kb fragments in each case) and probing with 5-P_1 (Fig. 1A and 7A) and 2-S_1P_2 (Fig.

TABLE 1. Level of genomic methylation in MNNG-induced TK$^+$ cell lines derived from RJK92

Cell line	TK enzymatic activity[a]	% of dCyds methylated[b]
RJK92	TK$^-$	1.81
4	Low TK$^+$	1.81
9	Low TK$^+$	1.76
15	Low TK$^+$	1.98
18	High TK$^+$	0.55
21	High TK$^+$	0.40
22	High TK$^+$	0.52

[a] As shown in Fig. 3, cell lines were grouped into TK$^-$ (<0.4 U), low enzyme activity (8-16 U), and high enzyme activity (>32 U) classes.

[b] Level of genomic methylation was measured by HPLC separation of labeled nucleosides as described in Materials and Methods.

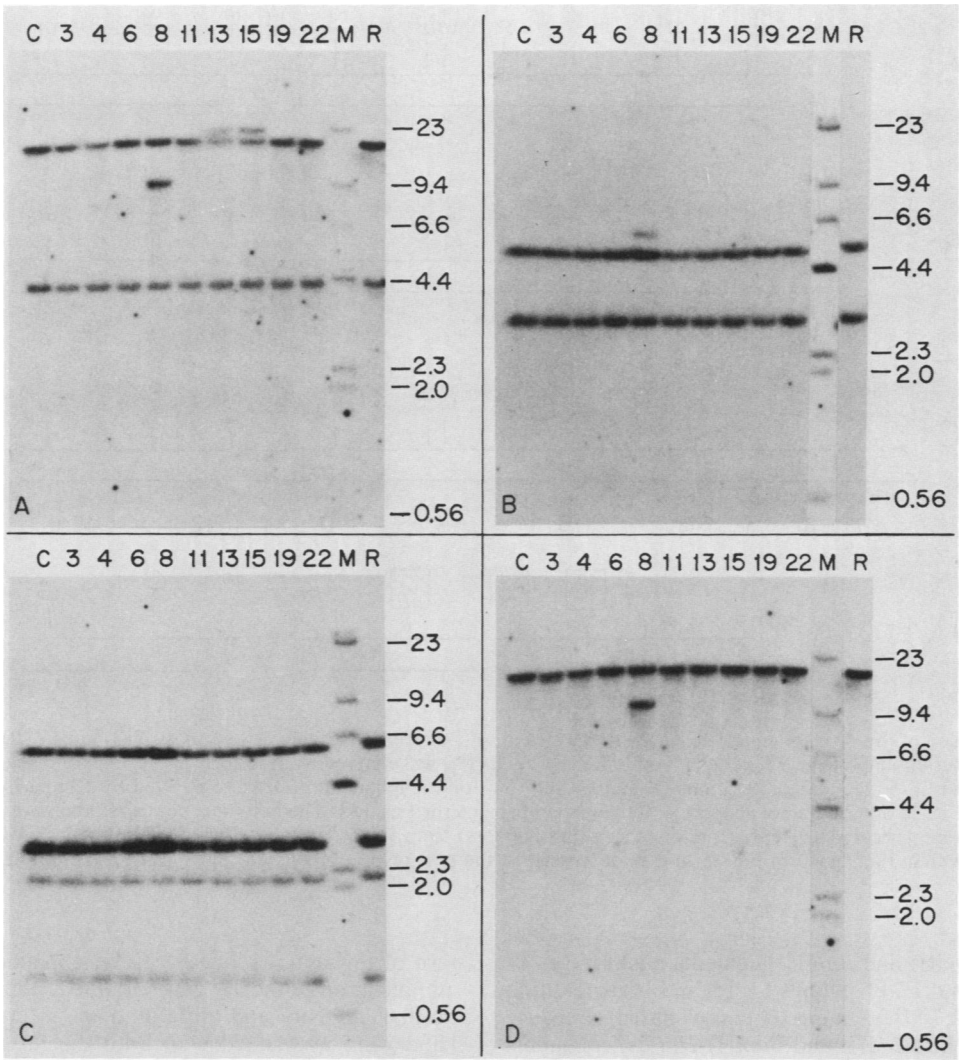

FIG. 7. Structural analysis of the far-5′ flanking (A), 5′ transcribed (B), 3′ transcribed (C), and far-3′ flanking (D) regions of the *TK* gene in MNNG-induced HAT^r derivatives of RJK92 cells. DNA samples (10 μg) from RJK92 (lane R), HAT^r TK$^-$ line C, low-activity TK$^+$ lines 3, 4, 6, 8, 11, 13, and 15, and high-activity TK$^+$ lines 19 and 22 were digested with *Hin*dIII (A and D) or with *Hin*cII and *Xmn*I (B and C), electrophoresed in 0.75% agarose gels, and blotted. Blots were hybridized to probes 5-P_1 (A), 5-NA (B), B-EH_3 (C), and 2-S_1P_2 (D). (The locations of these probes are shown in Fig. 1.) Processed gene fragments were detected in panel A as 4.2-kb bands and in panel C as 2.2- and 0.86-kb bands (data not shown). Lane M contains an end-labeled *Hin*dIII digest of λ DNA. Fragment sizes are shown in kilobases.

1A and 7D). Exon-containing probes 5-P_1 and B-EH_3 also hybridized to additional fragments (4.2-kb band in Fig. 7A and 2.2- and 0.9-kb bands in Fig. 7C), which we attribute to a homologous processed pseudogene (data not shown).

Fifteen low-activity TK$^+$ lines, three high-activity TK$^+$ lines, 10 HAT^r TK$^-$ lines, and RJK92 were examined by this restriction endonuclease analysis (Fig. 7 and data not shown). The limits of resolution of this analysis were estimated from the widths of bands at short exposure times to be about 0.2 kb for fragments smaller than 6 kb and about 1.3 kb for the 15.5-kb fragments. Five of 15 low-activity TK$^+$ lines demonstrated altered digestion patterns, while the high-activity TK$^+$ lines and TK$^-$ controls did not have any detectable changes in digestion patterns compared with that of RJK92. The altered restriction patterns were attributed to four instances of a far-5′ sequence alteration and one instance of a low-copy amplification (see below).

Structural alterations in the far-5′ region. The altered digestion patterns in four low-activity lines can be explained by a structural alteration in the far-5′ region of one copy of the *TK* gene. In lines 13, 15, and 16, a new far-5′ band of 19 kb appeared, while the expected 5′ band of 15.5 kb decreased in intensity (Fig. 7A; data not shown for line 16). There were no changes in digestion patterns further downstream (i.e., from the *Hin*cII site at −3.3 to the *Hin*dIII site at +27) in these cell lines (Fig. 7B, C, and D). By reducing the agarose concentration to 0.5% and thereby increasing the resolution of high-molecular-weight bands (0.8-kb limit at 15.5 kb), we reexamined the cell lines. On the higher-resolution gel, we detected a new far-5′ band of 16.5 kb as well as the normal 15.5-kb band in low-activity line 7 (data not shown).

The far-5′ alterations were further characterized by digesting DNA from lines 7, 13, 15, and 16 with *Hin*dIII and a second restriction enzyme and hybridizing with 5-P_1 or 5-NA. Following double digestion with *Hin*dIII and *Xmn*I (or *Sst*I), the digestion patterns were indistinguishable from that of RJK92 (data not shown); we conclude that the 3′ boundaries of the sequence alterations are 5′ to the *Xmn*I site at position −5.8 (Fig. 8B and 8C). In contrast, double

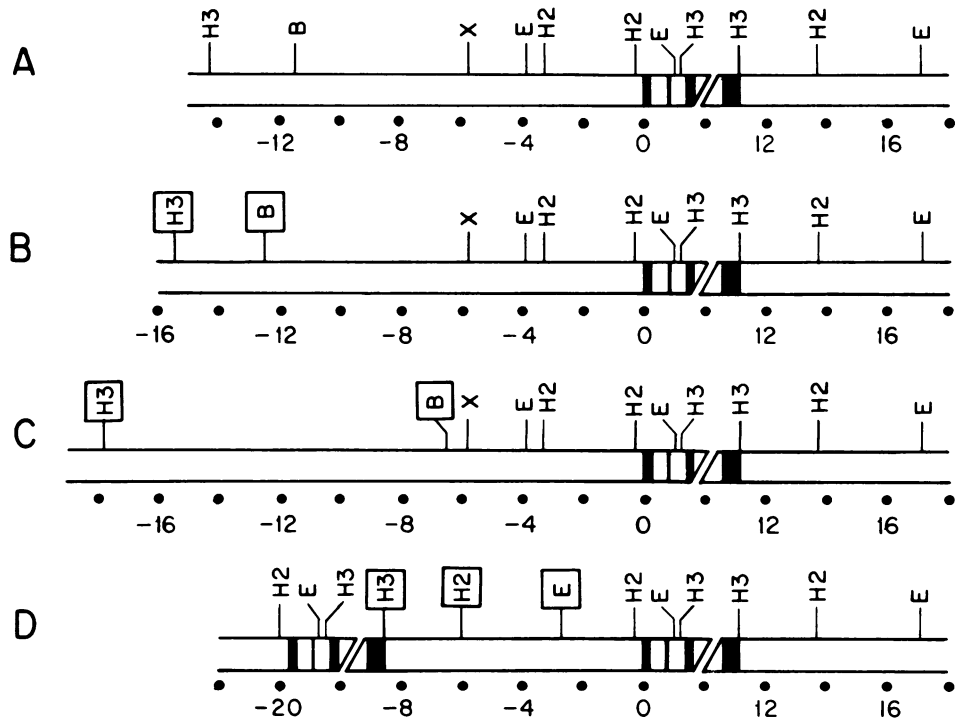

FIG. 8. Comparison of the *TK* gene in RJK92 (A) with the structurally altered *TK* gene in low-activity TK^+ lines 7 (B), 13, 15, and 16 (C), and 8 (D). The restriction map of the *TK* gene in parental RJK92 cells (A) was derived as described in the legend to Fig. 1, and the maps of the *TK* gene with the far-5′ sequence alterations (B and C) and low-copy amplification (D) were derived by comparison of Southern blot hybridization data (Fig. 7; other data not shown) with the map in panel A (or Fig. 1A). The first, second, third, and seventh exons are shown as solid boxes. The numerical scale represents distances (in kilobases) from the approximate origin of transcription. Restriction enzyme abbreviations are given in the legend to Fig. 1. In the TK^+ variants, the new restriction enzyme sites in the 5′ region have been enclosed in squares.

digestion with *Hin*dIII and *Bam*HI yielded a novel fragment (13.7 kb in line 7 and 7.7 kb in lines 13, 15, and 16) in addition to the expected 12.7-kb fragment (data not shown). Because the sizes of both the *Hin*dIII and *Bam*HI-*Hin*dIII fragments were affected by the far-5′ alteration, this alteration was not a single point mutation. In line 7, in which both the *Hin*dIII and *Bam*HI sites were shifted 1 kb upstream (Fig. 8B), the most likely sequence alteration is a 1-kb insertion between positions −5.8 and −11.5; however, a translocation, deletion, or larger insertion is also possible. In cell lines 13, 15, and 16, the new *Hin*dIII site mapped at position −17.8, while the new *Bam*HI site mapped at position −6.5 (Fig. 8C). The sequence changes in these three lines can be attributed to either an insertion (3.5 kb or larger than 11.3 kb) between positions −5.8 and −6.5, a translocation whose breakpoint occurs between these positions, or a deletion starting at a point between these positions and extending upstream past position −14.3. Although these three lines appear to contain the same rearrangement, we cannot yet determine whether there is a hot spot for rearrangement because the three lines were isolated from the same MNNG-treated culture and may therefore be derived from the same TK^+ variant cell.

To determine whether the far-5′ alteration occurs in the absence of *TK* activation, we examined 10 MNNG-induced HAT^r TK^- derivatives of RJK92 on the high-resolution gel. After digestion with *Hin*dIII and hybridization with 5-NA, we did not find any instance of a far-5′ alteration (data not shown). We therefore suggest that the structural change in the far-5′ region is associated with MNNG-induced *TK* activation and not with generalized MNNG damage.

Low-copy tandem amplification. The altered digestion pattern of low-activity line 8 can be explained by a low-copy amplification of the *TK* gene. In line 8, the expected band of normal intensity and an additional lower-molecular-weight band were associated with both the far-5′ and 3′ flanking regions (Fig. 7A and D). In the 3′ transcribed and nearby flanking regions (Fig. 7C, lane 8), only the expected bands were present; these bands, when examined after short exposure times, demonstrated low but detectable increases in intensity (data not shown). These data suggest that a sequence within the region bounded by the *Hin*dIII sites at −14 and +27 (Fig. 1A) was amplified to a small degree. The normal pattern in Fig. 7C, lane 8, indicates that the 3′ boundary of the locus of amplification was downstream of the *Hin*cII site at +13.7. The presence of an additional band in Fig. 7B, lane 8, indicates that the 5′ boundary of the locus of amplification was downstream of the *Hin*cII site at −3.3 but upstream of the probe 5-NA sequence. When the new *Eco*RI (data not shown), *Hin*cII, and *Hin*dIII sites of this amplified *TK* sequence were mapped in the 5′ flanking region (to positions −2.4, −6.2, and −8.7, respectively) (Fig. 8D), the relative spacing of these three new sites was comparable to that of the normal *Eco*RI, *Hin*cII, and *Hin*dIII sites in the 3′ flanking region (at positions +17.1, +13.7, and +11.1, respectively). These mapping data are consistent with the presence of a tandem arrangement of the amplified *TK* gene copies (Fig. 8D). This association of a tandem low-copy amplification with activation of an unexpressed gene differs from the results of previous studies, which found that an active gene was amplified to produce a higher level of drug resistance (34).

Methylation analysis of structurally altered genes. Because

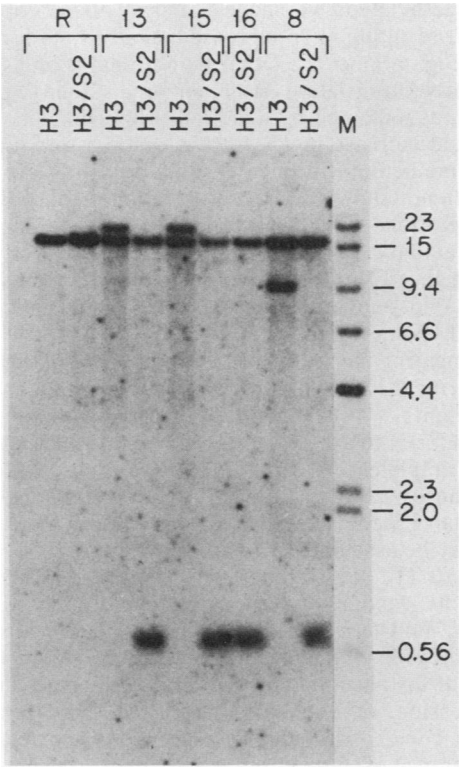

FIG. 9. Methylation analysis of the normal and structurally altered *TK* gene copies in the low-activity TK$^+$ variants with far-5′ sequence alterations or low-copy amplification. DNA samples (10 μg) from RJK92 (R) and low-activity TK$^+$ lines 8, 13, 15, and 16 were digested with *Hin*dIII alone or *Hin*dIII and *Sst*II, electrophoresed in a 0.75% agarose gel, and blotted. The blot was hybridized to probe 5-Sm. (The locations of this probe and the *Sst*II sites are shown in Fig. 5B.) Lane M contains a mixture of an end-labeled *Hin*dIII digest of λ DNA and an end-labeled *Xho*I digest of λ DNA.

5′ demethylation was absolutely correlated with *TK* expression, we investigated whether the structurally altered *TK* gene copy was demethylated in the low-activity *TK*$^+$ lines with detectable structural alterations. DNA from lines 13, 15, and 16 (with the far-5′ alteration) and line 8 (with the low-copy amplification) was digested with *Hin*dIII and the methylation-sensitive restriction enzyme *Sst*II. (A 6-bp-recognition-site methylation-sensitive enzyme was selected to reduce the probability of encountering a demethylated site in the far upstream region of RJK92.) When the cloned 5′ *TK* sequence was digested with *Sst*II and *Hin*dIII and hybridized to probe 5-Sm, we detected the expected 0.7-kb fully demethylated *Sst*II fragment (Fig. 5B; hybridization data not shown). The 15.5-kb *Hin*dIII fragment in RJK92 was resistant to *Sst*II digestion, confirming the methylated status of the *TK* gene in RJK92 (Fig. 9). In lines 13, 15, and 16, digestion of the normal 15.5-kb and novel 19-kb *Hin*dIII fragments with *Sst*II resulted in the disappearance of only the 19-kb band and the appearance of the 0.7-kb *Sst*II fragment. Similarly, the novel 10-kb *Hin*dIII fragment in line 8 was susceptible to *Sst*II digestion, while the normal fragment was resistant. Therefore, in the lines with a structurally altered copy of the *TK* gene, the *Sst*II sites in the 5′ region of the altered copy were demethylated. We further conclude that at least one (and probably all) of the normal *TK* gene copies in these cell lines have methylated *Sst*II sites in the 5′ region. (We have determined that there are two to four copies of the *TK* gene per RJK92 cell [data not shown].)

Analysis of spontaneous TK$^+$ variants. The mechanism of spontaneous activation of the *TK* gene was investigated by enzymatic, methylation, and structural analyses of three spontaneous TK$^+$ clones. Two of these cell lines expressed low TK enzymatic activity and one expressed high activity (data not shown). All three lines demonstrated focal *TK* gene demethylation; only a subset of the *TK* gene copies was demethylated (at *Hpa*II and *Hha*I sites), and the ethidium bromide-stained agarose gels did not show evidence of genomic hypomethylation (data not shown). Furthermore, there were no far-5′ rearrangements of the *TK* gene in these lines, but one low-activity line did demonstrate amplification of the *TK* gene (data not shown). Therefore, spontaneous *TK* gene activation in RJK92 cells is predominantly associated with a focal event which does not involve 5′ gene rearrangements. Although genomic hypomethylation and 5′ gene rearrangements may occur spontaneously at a lower frequency, the MNNG-induced 50-fold increase in HAT^r variants (which cannot be explained by selection) indicates that carcinogen action is responsible for the genomic hypomethylation, rearrangements, and the majority of the focal *TK* gene demethylation events. The relationship of carcinogen action and *TK* gene amplification is unclear.

DISCUSSION

As a model of the activation of a quiescent gene by a chemical carcinogen, we have developed a cell culture system in which MNNG activates *TK* expression and thereby induces HAT^r. Carcinogen treatment of TK$^-$ HAT^s RJK92 hamster cells induced a high frequency of phenotypically stable HAT^r derivatives. This high rate of conversion is similar to the rate of induction of cadmium resistance in mouse S49 cells by chemical carcinogens or UV radiation (24). The great majority of HAT^r derivatives expressed TK enzymatic activity which was absolutely correlated with demethylation of the 5′ region of the *TK* gene and the appearance of a TK mRNA of the appropriate size (1,400 nucleotides). In four of five high-activity TK$^+$ variants, there was extensive genomic hypomethylation in addition to *TK* gene demethylation. Also, 4 of 15 low-activity TK$^+$ variants had a translocation, insertion, or deletion in the far-5′ region of the *TK* gene, and a fifth line had a tandem low-copy amplification of the *TK* gene. Therefore, we conclude that MNNG can activate *TK* expression in RJK92 cells by several different mechanisms. Activation of a low level of TK activity is associated with focal gene demethylation and sequence alterations 5′ to the *TK* gene. In contrast, activation of a high level of TK activity is associated with demethylation throughout the genome.

In approximately 20% of the HAT^r derivatives of RJK92, HAT^r resulted from a mechanism other than *TK* expression, as indicated by the lack of TK enzyme activity, absence of the 1,400-nucleotide TK mRNA, and fully methylated status of the *TK* gene. Possible alternative mechanisms for HAT^r are decreased membrane transport of aminopterin (14), decreased intracellular polyglutamylation of aminopterin, which would lower the potency of the drug (27), and changes such as gene amplification of the locus encoding the target enzyme, dihydrofolate reductase (34).

By monitoring the methylation status of the 5′ region of the *TK* gene, we have demonstrated that TK activation is

associated with changes at the *TK* gene (Fig. 5A). Although these methylation changes may be related to sequence alterations that were not detected by our restriction endonuclease analysis, several mechanisms have been proposed by which carcinogen damage can lead directly to demethylation. Methylation of dCyd residues in DNA repair patches following excision repair is slow and perhaps incomplete (17). In addition, in vitro experiments have indicated that numerous carcinogen adducts of DNA are capable of inhibiting the activity of DNA methyltransferases (36). Either mechanism could prevent the cell from maintaining its specific methylation pattern; if the cell then divided prior to restoration of this pattern, an inheritable loss of methylation could result. When such demethylation involves key sites or regions of the *TK* gene, the new information may permit *TK* expression by modulating the binding of sequence-specific regulatory factors or by altering the overall chromatin structure (5).

An alternative explanation proposes that the observed methylation changes might be secondary to a mutagenic event (such as a point mutation or rearrangement). A mutation in a regulatory region may be able to activate expression which leads to demethylation, or the mutation may promote demethylation which leads to expression. However, the ability of azaCyd (32) to activate *TK* expression at a high frequency in RJK92 cells (12) indicates that the inactivity of the *TK* gene is not the result of a mutation. Therefore, if activating mutations are induced by MNNG, they do not act by reverting an inactivating mutation in the parental line.

In all the low-activity TK^+ lines tested, we detected demethylation in only a subset of the *TK* gene copies, and in four of these lines this demethylation was further localized to a structurally altered *TK* gene copy (Fig. 9). If carcinogen-induced *TK* activation involved changes in the set of *trans*-acting factors, one would expect that all *TK* gene copies would be demethylated and activated. Therefore, our data support the hypothesis that, for the activation of low levels of *TK* expression, the carcinogen acted directly at or near the *TK* gene.

In the high-activity TK^+ lines, demethylation affected all *TK* gene copies and occurred in the 3′ region as well as the 5′ region of the gene. Furthermore, there was a large decrease in the genomic methyl-dCyd content in these lines. These results suggest that *TK* gene demethylation is part of an extensive genomic demethylation process. The persistence of extensive genomic hypomethylation in the absence of MNNG contrasts with the transient decrease in genomic methylation following azaCyd or 5-aza-dCyd treatment (believed to be the result of widespread inhibition of methyltransferase activity) (8, 20, 33). Furthermore, the finding of a bimodal rather than a continuous distribution of methyl-dCyd contents in MNNG-treated cell lines (Table 1) suggests that the genomic hypomethylation results from carcinogen action at a specific gene locus and not from many individual carcinogen-induced demethylation events. Carcinogen damage of a gene coding for DNA methyltransferase(s) or protein cofactor(s) involved in DNA methylation may inactivate or decrease the activity of the methylation apparatus. Alternatively, alterations in genes coding for the enzymes involved in *S*-adenosylmethionine synthesis could lead to a constitutively low level of the methyl group donor and resulting decreased methyltransferase activity.

The high level of TK enzyme activity in cell lines with extensive genomic hypomethylation can be explained by several different hypotheses. Because all the *TK* gene copies were demethylated, we suggest that all these copies were activated, resulting in an increased steady-state level of TK mRNA (Fig. 4, lane 22). Other alterations, such as changes in TK mRNA translation or TK enzyme stability, may have occurred, as indicated by a lack of proportionality between the twofold increase in TK mRNA and 5.5-fold increase in TK enzyme activity in line 22 relative to low-activity TK^+ lines (data not shown). These translational and posttranslational alterations may also be partly responsible for the high enzyme activity (3-fold higher TK enzyme activity and 1.5-fold higher TK mRNA level relative to low-activity TK^+ lines; data not shown) in line 19, which did not demonstrate genomic hypomethylation.

By comparing the restriction endonuclease patterns of the *TK* gene in RJK92 with those of our carcinogen-induced TK^+ variants, we identified four lines with a sequence alteration far-5′ to the *TK* gene and one line with a low-copy *TK* gene amplification (Fig. 7 and 8); all five of these lines were in the low-activity TK^+ group. Several findings suggest that the far-5′ sequence changes and the low-copy amplification may be associated with the process of TK activation. First, in 10 TK^- HAT^r lines derived from MNNG-treated RJK92 cells, we did not detect any structural changes in the *TK* locus. Furthermore, in the lines with the structurally altered *TK* gene, the altered gene copy was demethylated. Because of the absolute correlation of 5′ demethylation and TK expression, we conclude that these altered gene copies are active copies. Although TK activation is correlated with the appearance of these structural changes, it is not possible to determine whether the appearance of the sequence alteration preceded (and possibly caused) or followed the activation event.

Several hypotheses may explain how a structural change could activate a quiescent gene. A translocation, deletion, or insertion may bring the *TK* gene into proximity with new *cis*-acting positive regulatory influences, such as enhancers. These elements can act on promoters which are several kilobases away (2) and have been implicated in immunoglobulin gene activation following gene rearrangement (9). Transcriptional enhancers are also postulated to be responsible for c-*myc* activation after retroviral gene insertion adjacent to the oncogene in chicken B-cell lymphomas or after transposition of the oncogene into the immunoglobulin domain in human Burkitt's lymphomas (9).

Another *cis*-acting positive regulatory influence may be an active chromatin structure. The ability of the chromatin of the B-cell immunoglobulin domain to exert a positive regulatory influence on the transposed c-*myc* gene has been proposed to explain the variability of translocation breakpoints in Burkitt's lymphoma (19). Similarly, a translocation, insertion, or deletion might bring the inactive *TK* gene next to an active region, which could then promote demethylation or direct the assembly of an active chromatin structure about the *TK* gene.

The relevance of carcinogen-induced genomic hypomethylation to the process of neoplasia is supported by previous reports of decreased genomic methylation levels in chemically induced and spontaneous tumors (11, 21). Furthermore, our finding of carcinogen-induced sequence alterations 5′ to the *TK* gene is reminiscent of the chromosomal rearrangements identified in several neoplasms (19, 31). Thus, while we do not believe that TK activation is involved in the process of neoplasia, this model cell culture system has provided insights into the molecular basis of carcinogen action and should facilitate detailed analysis of some of the genomic changes which occur during carcinogenesis.

ACKNOWLEDGMENTS

We thank Thomas Caskey, Raymond Fenwick, and John Lewis for their generous assistance and advice; Teresa Hawley and Eileen Walsh for technical assistance; and John Burch, Steven Dresler, Andrew Godwin, Russell Lebovitz, Vincent Reynolds, Jesse Summers, and Thomas Winokur for their thoughtful comments.

This investigation was supported by Public Health Service grant CA39392 and by National Institutes of Health Research Service Award GM-07200, Medical Scientist, from the National Institutes of Health. F.G.B. and C.A.M. are trainees of the Washington University Medical Scientist Training Program, St. Louis, MO 63110.

LITERATURE CITED

1. **Arcos, J. C., Y. T. Woo, and M. F. Argus.** 1982. Chemical induction of cancer—structural bases and biological mechanisms, vol. 3A, p. 148–325. Academic Press, Inc., New York.
2. **Banerji, J., S. Rusconi, and W. Schaffner.**1981. Expression of a β-globin gene is enhanced by remote SV40 DNA sequences. Cell **27**:299–308.
3. **Barr, F. G., M. B. Kastan, and M. W. Lieberman.** 1985. Distribution of 5-methyldeoxycytidine in products of staphylococcal nuclease digestion of nuclei and purified DNA. Biochemistry **24**:1424–1428.
4. **Chu, E. H. Y., and T. Ho.** 1970. Forward and reverse mutations in the resistance of Chinese hamster cells to 5-bromodeoxyuridine. Mamm. Chromosomes Newl. **11**:58–59.
5. **Doerfler, W.** 1983. DNA methylation and gene activity. Annu. Rev. Biochem. **52**:93–124.
6. **Farber, E.** 1981. Chemical carcinogenesis. N. Engl. J. Med. **305**:1379–1389.
7. **Fenwick, R. G., and C. T. Caskey.** 1975. Mutant Chinese hamster cells with a thermosensitive hypoxanthine-guanine phosphoribosyltransferase. Cell **5**:115–122.
8. **Flautau, E., F. A. Gonzales, L. A. Michalowsky, and P. A. Jones.** 1984. DNA methylation in 5-aza-2′-deoxycytidine-resistant variants of C3H 10T1/2 C18 cells. Mol. Cell. Biol. **4**:2098–2102.
9. **Gillies, S. D., S. L. Morrison, V. T. Oi, and S. Tonegawa.** 1983. A tissue-specific transcription enhancer element is located in the major intron of a rearranged immunoglobulin heavy chain gene. Cell **33**:717–728.
10. **Gillin, F. D., D. J. Roufa, A. L. Beaudet, and C. T. Caskey.** 1972. 8-Azaguanine resistance in mammalian cells. I. Hypoxanthine-guanine phosphoribosyltransferase. Genetics **72**:239–252.
11. **Goelz, S. E., B. Vogelstein, S. R. Hamilton, and A. P. Feinberg.** 1985. Hypomethylation of DNA from benign and malignant human colon neoplasms. Science **228**:187–190.
12. **Harris, M.** 1982. Induction of thymidine kinase in enzyme-deficient Chinese hamster cells. Cell **29**:483–492.
13. **Harris, M., and K. Collier.** 1980. Phenotypic evolution of cells resistant to bromodeoxyuridine. Proc. Natl. Acad. Sci. USA **77**:4206–4210.
14. **Hill, B., B. D. Bailey, J. C. White, and I. D. Goldman.** 1979. Characteristics of transport of 4-amino antifolates and folate compounds by two lines of L5178Y lymphoblasts, one with impaired transport of methotrexate. Cancer Res. **39**:2440–2446.
15. **Ivarie, R., and J. A. Morris.** 1986. Activation of a nonexpressed hypoxanthine phosphoribosyltransferase allele in mutant H23 HeLa cells by agents that inhibit DNA methylation. Mol. Cell. Biol. **6**:97–104.
16. **Jones, P. A.** 1985. Altering gene expression with 5-azacytidine. Cell **40**:485–486.
17. **Kastan, M. B., B. J. Gowans, and M. W. Lieberman.** 1982. Methylation of deoxycytidine incorporated by excision-repair synthesis of DNA. Cell **30**:509–516.
18. **King, H. W. S., and P. Brookes.** 1985. On the mechanism of induction of resistance to 6-thioguanine in Chinese hamster V79 cells by 3-methylcholanthrene-diolepoxide. Carcinogenesis. **6**:1471–1476.
19. **Klein, G., and E. Klein.** 1985. Evolution of tumours and the impact of molecular oncology. Nature (London) **315**:190–195.
20. **Krawisz, B. R., and M. W. Lieberman.** 1984. Methylation of deoxycytidine in replicating cells treated with ultraviolet radiation and chemical carcinogens. Carcinogenesis **5**:1141–1144.
21. **Lapeyre, J., M. S. Walker, and F. F. Becker.** 1981. DNA methylation and methylase levels in normal and malignant mouse hepatic tissues. Carcinogenesis **2**:873–878.
22. **Lewis, J. A., K. Shimuzu, and D. Zipser.** 1983. Isolation and preliminary characterization of the Chinese hamster thymidine kinase gene. Mol. Cell. Biol. **3**:1815–1823.
23. **Lieberman, M. W., L. R. Beach, and R. D. Palmiter.** 1983. Ultraviolet radiation-induced metallothionein-I gene activation is associated with extensive DNA demethylation. Cell **35**: 207–214.
24. **MacArthur, C. A., R. Ramabhadran, A. K. Godwin, R. M. Lebovitz, and M. W. Lieberman.** 1985. Chemical carcinogens induce cadmium resistance and activate metallothionein genes in cadmium sensitive S49 mouse cells. Carcinogenesis **6**: 887–892.
25. **Maniatis, T., E. F. Fritsch, and J. Sambrook.** 1982. Molecular cloning: a laboratory manual. Cold Spring Harbor Laboratory, Cold Spring Harbor, N.Y.
26. **Marshall, C. J., K. H. Vousden, and D. H. Phillips.** 1984. Activation of c-Ha-*ras*-1 proto-oncogen by *in vitro* modification with a chemical carcinogen, benzo(a)pyrene diol-epoxide. Nature (London) **310**:586–589.
27. **Matherly, L. H., M. K. Voss, L. A. Anderson, D. W. Fry, and I. D. Goldman.** 1985. Enhanced polyglutamylation of aminopterin relative to methotrexate in the Ehrlich ascites tumor cell *in vitro*. Cancer Res. **45**:1073–1078.
28. **Orlofsky, A., and L. A. Chasin.** 1985. A domain of methylation change at the albumin locus in rat hepatoma cell variants. Mol. Cell. Biol. **5**:214–225.
29. **Palmiter, R. D., H. Y. Chen, and R. L. Brinster.** 1982. Differential regulation of metallothionein-thymidine kinase fusion genes in transgenic mice and their offspring. Cell **29**:701–710.
30. **Roufa, D. J., B. N. Sadow, and C. T. Caskey.** 1973. Derivation of TK^- clones from revertant TK^+ mammalian cells. Genetics **75**:515–530.
31. **Rowley, J. D.** 1982. Identification of the constant chromosome regions involved in human hematologic malignant disease. Science **216**:749–751.
32. **Taylor, S. M., P. A. Constantinides, and P. A. Jones.** 1984. 5-Azacytidine, DNA methylation, and differentiation. Curr. Top. Microbiol. Immunol. **108**:115–127.
33. **Taylor, S. M., and P. A. Jones.** 1982. Mechanism of action of eukaryotic DNA methyltransferase—use of 5-azacytosine-containing DNA. J. Mol. Biol. **162**:679–692.
34. **Tlsty, T. D., P. C. Brown, and R. T. Schimke.** 1984. UV radiation facilitates methotrexate resistance and amplification of the dihydrofolate reductase gene in cultured 3T6 mouse cells. Mol. Cell. Biol. **4**:1050–1056.
35. **Vogelstein, B., and D. Gillespie.** 1979. Preparative and analytical purification of DNA from agarose. Proc. Natl. Acad. Sci. USA **76**:615–619.
36. **Wilson, V. L., and P. A. Jones.** 1983. Inhibition of DNA methylation by chemical carcinogens *in vitro*. Cell **32**:239–246.